

# Effects of Attractive correlation on Topological Flat-bands Model

Chun-Li Zang,<sup>1,\*</sup> Jing He,<sup>2</sup> and Ya-Jie Wu<sup>1</sup>

<sup>1</sup>Department of Physics, Beijing Normal University, Beijing, 100875, P. R. China

<sup>2</sup>Department of Physics, Hebei Normal University, Hebei, 050024, P. R. China

In this paper, we study the effects of attractive correlation on the topological insulator (*TI*) with topological flat-bands using an extended attractive Kane-Mele-Hubbard model (KMHM). In the KMHM, we found a quantum phase transition from *TI* to the superconductor (*SC*) state upon the increasing of the attractive Hubbard interaction  $U$  at the mean field level. This type of *SC* phase transition is different from the traditional *SC* phase transition which develops from the gapless Fermi Liquid. Cooperon-type gapped excitations exist in the *TI* side near this type of *SC* phase transition.

## I. INTRODUCTION

The integer quantum Hall (IQH) effect was first observed in a two dimensional (2D) electron gas subjected to strong perpendicular magnetic field[1]. This effect provides the first example of topological states that beyond the Landau symmetry breaking paradigm. After this observation, Haldane, in 1988, proposed a model (the Haldane model) and he found a state which also has the IQH effect in this model but the realization of this state doesn't need the external magnetic field[2]. The Haldane model describe a system spinless fermions and the time reversal symmetry is broken in this model by its complex NNN hoppings. The state that Haldane found is also a topological one. The two type topological states we mentioned above that support IQH effect could be characterized by an topological invariant - TKNN number (the Chern number)[3]. Following the lesson from the Haldane model, people wonder naturally that whether the fractional quantum Hall (FQH) effect could also be realized in a model without external magnetic field. Recently, models with topologically nontrivial flat-bands (TFBs) were found to be an promising candidate to realize FQH effect without external magnetic field[5-7].

Along with the IQH and FQH states in which time-reversal symmetry breaking is required, time-reversal symmetry protected topological states of matters are also discovered in the quantized spin Hall effect (QSH)[8, 9]. People called them  $Z_2$  topological insulator (*TI*) state. The typical model for the  $Z_2$  topological insulator is the Kane-Mele (KM) model[9]. Recently, the correlated effects in *TI* states are studied by various groups with the Kane-Mele-Hubbard model as the starting point[11, 12].

In this paper, we investigate the effects of attractive interaction to a TFBs system using an attractive Kane-Mele-Hubbard model on the honeycomb lattice:  $H_{\text{KMHM}}$ . There are two important parts in  $H_{\text{KMHM}}$ :  $H_{\text{EKHM}}$  and  $H_U$ , see Eq.(1). In the original KM model, the authors generalizes Haldane's model [2] to include spin with time reversal invariant spin-orbit interactions[9]. So the KM

model is a free model.  $H_{\text{EKHM}}$  is the free limit ( $U = 0$ ) of  $H_{\text{KMHM}}$  and is a general case of KM model i.e., the next-nearest-neighbor (NNN) hoppings for the spin- $\uparrow$  and spin- $\downarrow$  electrons are complex valued and complex conjugate to each other in  $H_{\text{EKHM}}$ . So the Kane-Mele model is a special case of  $H_{\text{EKHM}}$  i.e., when the complex valued NNN hoppings is purely imaginary or the Haldane phase  $\hat{\phi}_{ij}$  in Eq.(2) is  $\pi/2$ . There are particle-hole symmetry in the half-filling original Kane-Mele model i.e., when the complex valued NNN hoppings is purely imaginary it reduce to a spin-orbit interactions[4]. So there are no particle-hole symmetry in  $H_{\text{EKHM}}$  except  $\hat{\phi}_{ij} = \pi/2$ . If we varying the Haldane phase  $\hat{\phi}_{ij}$  there exist a so called TFBs limit in  $H_{\text{EKHM}}$  [5-7], see Fig.1(b).

Generally for the system with flat-bands, the kinetic energy will be quite suppressed and the interaction becomes highly relevant. In this paper,  $H_U$  in  $H_{\text{KMHM}}$  is treated by self consisted mean field method, at this level we find a *TI* - *SC* quantum phase transition as the Hubbard interaction strength increases beyond a critical value  $U_c$  in the  $H_{\text{KMHM}}$  model, see Fig.4. In this type *SC* phase transition, there is a kind of Cooperon-type excitations in the insulator side near the *SC* phase transition and the Cooperon-type excitations are gapped before its condensation [17, 18].

## II. TOPOLOGICAL FLAT-BAND MODEL

The Hamiltonian that we study in this paper is  $H_{\text{KMHM}}$ , the attractive Kane-Mele-Hubbard model which can be writed as:

$$H_{\text{KMHM}} = H_{\text{EKHM}} + H_U - \mu \sum_{i,\sigma} \hat{c}_{i\sigma}^\dagger \hat{c}_{i\sigma}, \quad (1)$$

where  $\sigma = \uparrow, \downarrow$  denotes the spin degree freedom,  $H_U = -U \sum_i \hat{n}_{i\uparrow} \hat{n}_{i\downarrow}$  represent the on-site Hubbard type attractive interaction,  $\mu$  is the chemical potential. We call  $H_{\text{EKHM}}$  the extended KM model whose Hamiltonian is

\*zangzys@mail.bnu.edu.cn

written as:

$$H_{\text{EKM}} = -t \sum_{\langle i,j \rangle, \sigma} \hat{c}_{i\sigma}^\dagger \hat{c}_{j\sigma} - t' \sum_{\langle\langle i,j \rangle\rangle, \sigma} e^{i\hat{\phi}_{ij}\hat{\sigma}_z} \hat{c}_{i\sigma}^\dagger \hat{c}_{j\sigma} \quad (2)$$

$$- t'' \sum_{\langle\langle\langle i,j \rangle\rangle\rangle, \sigma} \hat{c}_{i\sigma}^\dagger \hat{c}_{j\sigma} + h.c.$$

In  $H_{\text{EKM}}$ , the first term describes the nearest-neighbor (NN) hopping on the honeycomb lattice and its hopping strength  $t$  is set as the unit of energy in the rest of this paper. The second term describes the next-nearest-neighbor (NNN) hopping with a Haldane type complex strength  $t'e^{i\hat{\phi}_{ij}}$ , the phase factor in this term is spin depended, i.e.,  $e^{i\hat{\phi}_{ij}} = e^{i\phi}$  for spin  $\uparrow$  electron that hopping clockwise in the fundamental plaquette as shown by the blue arrow in Fig.1(a) and  $e^{i\hat{\phi}_{ij}} = e^{-i\phi}$  for spin  $\downarrow$  electron. This term recover the original spin-orbit coupling term of KM model when  $\phi = \pi/2$  (so here  $t'$  cannot be regarded as the spin-orbit interaction strength). This term also reduces  $H_{\text{EKM}}$ 's full spin rotational SU(2) symmetry to a U(1) symmetry. Thus there is time reversal symmetry (TRS) but no full spin rotation symmetry in  $H_{\text{EKM}}$ . The last term represents the next-next-nearest-neighbor (NNNN) hopping with strength  $t''$ , the energy bands of  $H_{\text{EKM}}$  could achieve a flat-bands limit with this term in it (more about this limit see below). In this paper, we consider the half-filling case of  $H_{\text{KMH}}$  i.e., the chemical potential  $\mu = 0$ .

The  $H_{\text{EKM}}$  model is the free limit ( $U = 0$ ) of the  $H_{\text{KMH}}$  model. In terms of the basis vector  $\Phi^\dagger(k) = [a_{k\uparrow}^\dagger, b_{k\uparrow}^\dagger, a_{k\downarrow}^\dagger, b_{k\downarrow}^\dagger]$ ,  $H_{\text{KMH}}$  could be expressed in a block-diagonal matrix form as:  $H_{\text{EKM}} = \sum_k \Phi^\dagger(k) H_0(k) \Phi(k)$  where

$$H_0(k) = I_0 C + \begin{pmatrix} \mathbf{h}_\uparrow \cdot \boldsymbol{\sigma} & 0 \\ 0 & \mathbf{h}_\downarrow \cdot \boldsymbol{\sigma} \end{pmatrix} \quad (3)$$

with  $\mathbf{h}_\uparrow = (h^x, h^y, h^z)$ ,  $\mathbf{h}_\downarrow = (h^x, h^y, -h^z)$ ,  $I_0$  is the  $4 \times 4$  unit matrix and  $\boldsymbol{\sigma}$  is the Pauli matrix that act on the A, B sublattice space of the bipartite honeycomb lattice. The three components of vector  $\mathbf{h}_{\uparrow(\downarrow)} = (\text{Re } \gamma(k), -\text{Im } \gamma(k), D)$ , where  $\gamma(k) = \xi(k) + \xi''(k)$  with  $\xi(k) = -t \sum_{i=1}^3 e^{ik \cdot \vec{a}_i}$  and  $\xi''(k) = -t'' \sum_{i=1}^3 e^{ik \cdot \vec{c}_i}$ , with  $\vec{a}_1 = (1/2, -\sqrt{3}/2)$ ,  $\vec{a}_2 = (1/2, \sqrt{3}/2)$ ,  $\vec{a}_3 = (-1, 0)$ .

$$C = -2t' \cos \phi_{ij} \sum_{i=1}^3 \cos[k \cdot \vec{b}_i]$$

$$D = -2t' \sin \phi_{ij} \sum_{i=1}^3 \sin[k \cdot \vec{b}_i] \quad (4)$$

with  $\vec{b}_1 = (3/2, -\sqrt{3}/2)$ ,  $\vec{b}_2 = (0, \sqrt{3})$ ,  $\vec{b}_3 = (-3/2, -\sqrt{3}/2)$ , see Fig.1(a). We set the lattice constant  $a = 1$  in the rest of the paper. The energy dispersion of the  $H_{\text{EKM}}$  can be founded by diagonalize  $H_0(k)$ :

$$E_n(k) = C \pm \sqrt{(h^x)^2 + (h^y)^2 + (h^z)^2}. \quad (5)$$

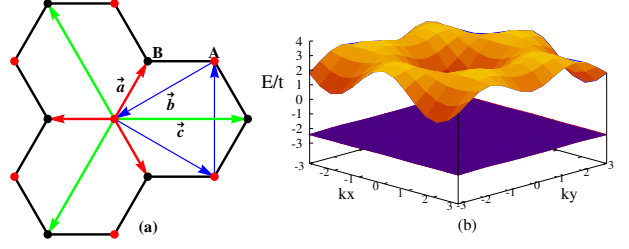


FIG. 1: (color online)(a) The honeycomb lattice consists of two sublattices: A (the red sites) and B (the black sites). The NN (red), NNN (blue) and NNNN (green) displacement vectors are denoted by  $\vec{a}$ ,  $\vec{b}$  and  $\vec{c}$  respectively. The arrow in  $\vec{b}$  also denote the positive phase direction of the complex factor  $e^{i\phi_{ij}}$  that company the NNN hopping. (b) The TFBs in the energy spectrum of the  $H_{\text{EKM}}$  with parameters:  $t'/t = 0.6$ ,  $t''/t = -0.58$ ,  $\phi_{ij} = 0.4\pi$ .

There are two energy bands in  $E_n(k)$ , both of them are doubly degenerate due to the spin degree freedom and have a flat-bands limit, i.e., with parameters:  $\phi = 0.4\pi$ ,  $t' = 0.6t$ ,  $t'' = -0.58t$  [6]. In this limit, the lower bands of  $E_n(k)$  will become flat, see Fig.1(b). The flatness ratio of the flat-bands in this limit (the ratio of the band gap over bandwidth) can reach about 50. we know that the NN and NNNN hopping energy  $\xi(k)$  and  $\xi''(k)$  are vanish at the two Dirac points:  $(2\pi/3, 2\pi/3\sqrt{3})$  and  $(2\pi/3, -2\pi/3\sqrt{3})$  in momentum space, but the NNN hopping energy  $\xi'_{a(b)}(k)$  dose not, just like the spin-orbit coupling term in KM model, it will opens an energy gap at those two Dirac points. So  $H_{\text{KMH}}$  is gapped in its free limit. We denote this energy gap as  $\Delta_{t'}$ , it's the bulk gap of the TI state since before  $H_{\text{KMH}}$  model entering the SC phase it is in a TI phase, the magnitude of  $\Delta_{t'}$  is related to  $t'$ . Thus we called  $\Delta_{t'}$  the bulk gap which playing the same role as the gap of semiconductor in [17].

In  $H_{\text{KMH}}$ 's flatband limit, the Chern number for the spin up and down electron that filled the two lowest bands of  $E_n(k)$  can be calculate in this way:

$$C_{\uparrow/\downarrow} = \frac{1}{4\pi} \int \mathbf{n} \cdot \left( \frac{\partial \mathbf{n}}{\partial k_x} \times \frac{\partial \mathbf{n}}{\partial k_y} \right) d^2k$$

The Chern number of spin  $\uparrow$  components electron is  $C_\uparrow = 1$  with  $\mathbf{n} = \mathbf{h}_\uparrow / |\mathbf{h}_\uparrow|$  and  $C_\downarrow = -1$  with  $\mathbf{n} = \mathbf{h}_\downarrow / |\mathbf{h}_\downarrow|$ , reflecting the TRS in  $H_{\text{EKM}}$ . The spin Chern number  $C_s = (C_\uparrow - C_\downarrow) / 2 = 1$  reflect the QSH in the free limit of  $H_{\text{KMH}}$  model[13].

This conclusion could be further verified by the presence of edge states in the energy spectrum of  $H_{\text{EKM}}$  when it's imposed a cylinder boundary condition with zigzag edges, i.e., we set periodic boundary condition along the system's  $x$ -direction and open boundary condition along the  $y$ -direction. The numerical results are depicted in Fig.2, from which we can see that there are topologically protected edge states, which is one of the signatures of topological states of matter. So in half-filling

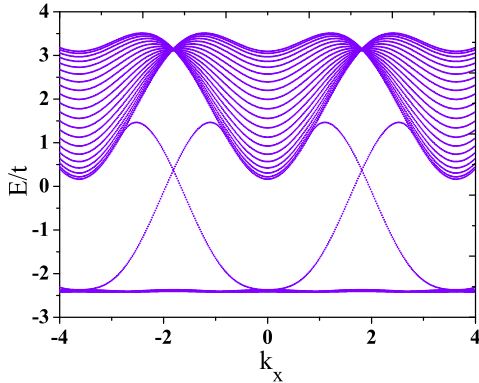


FIG. 2: (color online) The edge states of  $H_{\text{EKM}}$  in its flat-bands limit in a cylinder geometry with a zigzag edge. This is a typical edge states of TRS topological insulator which also reflecting the nontrivial topology of the flat-bands.

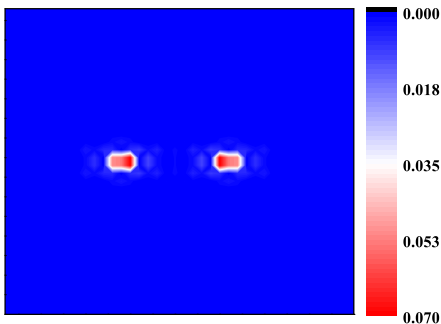


FIG. 3: (color online) The contour plots of the particle density distribution of the wave function of the zero-energy modes in coordinate space, this pair of zero-energy modes are bound to the  $\pi$ -fluxes. The values of particle density are indicated by color in this figure, the parameters are in  $H_{\text{KMH}}$ 's flat-bands limit.

and flat-bands limit, with the two lowest flat-bands are filled,  $H_{\text{EKM}}$  support the so called TFBs. Thus in the flat-bands limit of  $H_{\text{EKM}}$  model, it is a  $Z_2$  TI with TFBs as a consequence of the TRS in  $H_{\text{EKM}}$ .

On the other hand, the response of TI to topological defects such as:  $\pi$ -fluxes has also been suggested as a probe of the nontrivial topology of the  $Z_2$  TI [14]. Through numerical calculation, we really found that there are zero-energy modes in the energy spectrum if a pair of  $\pi$ -fluxes are adiabatically inserted into the  $H_{\text{EKM}}$  model in its flat-bands limit. From the particle density distribution in Fig.3, we can see that those zero-energy modes are really located around the  $\pi$ -fluxes in coordinate space. Those results imply that the  $H_{\text{EKM}}$  model's topological non trivial in its flat-bands limit.

### III. INTERACTING FLAT-BAND MODEL

In this section, we study the effects of attractive Hubbard type interaction of  $H_{\text{KMH}}$  model in the flat-bands limit of  $H_{\text{EKM}}$  with the mean field method. In this limit, the resulting mean field phase diagram of the  $H_{\text{KMH}}$  model could be seen from Fig.4(a). From Fig.4(a) we could see that the TI phase in the  $H_{\text{KMH}}$ 's free limit is unstable against an SC phase transition as the interaction strength increase beyond a finite critical value:  $U_c \simeq 3.03t$ .

According to the self-consistent mean field method, firstly we introduce an  $SC$  order parameter fields to decouple the Hubbard term  $H_U$  in  $H_{\text{KMH}}$ . The  $SC$  order parameter fields are defined as:  $\Delta_s = \langle \hat{c}_{i\uparrow} \hat{c}_{i\downarrow} \rangle$ . By the mean field approximation, we substitute  $\hat{c}_{i\uparrow}^\dagger \hat{c}_{i\downarrow}^\dagger = \langle \hat{c}_{i\uparrow}^\dagger \hat{c}_{i\downarrow}^\dagger \rangle + \delta^\dagger$  and  $\hat{c}_{i\uparrow} \hat{c}_{i\downarrow} = \langle \hat{c}_{i\uparrow} \hat{c}_{i\downarrow} \rangle + \delta$  into the Hubbard term  $H_U$  in Eq.(1), with  $\delta^\dagger = (\hat{c}_{i\uparrow}^\dagger \hat{c}_{i\downarrow}^\dagger - \langle \hat{c}_{i\uparrow}^\dagger \hat{c}_{i\downarrow}^\dagger \rangle)$  and  $\delta = (\hat{c}_{i\uparrow} \hat{c}_{i\downarrow} - \langle \hat{c}_{i\uparrow} \hat{c}_{i\downarrow} \rangle)$  two small quantities. We discard the second order terms of  $\delta^\dagger$  and  $\delta$ , then  $H_U$  could be decoupled into a bilinear form of  $\hat{c}_{i\sigma}^\dagger$  and  $\hat{c}_{i\sigma}$  as:

$$H_U = -U \sum_i \hat{n}_{i\uparrow} \hat{n}_{i\downarrow} \simeq -U \sum_i \left[ \Delta_s^\dagger \hat{c}_{i\downarrow} \hat{c}_{i\uparrow} + \Delta_s \hat{c}_{i\uparrow}^\dagger \hat{c}_{i\downarrow}^\dagger \right] + UN_s |\Delta_s|^2. \quad (6)$$

The honeycomb lattice's bipartite and translational invariant, so we could introduce the usual Fourier transformation to the electron creation (destruction) operator  $\hat{c}_{i\sigma}^\dagger$  ( $\hat{c}_{i\sigma}$ ) in  $H_{\text{KMH}}$  and we denote the fourier transform of  $\hat{c}_{i \in A, \sigma}^\dagger$  and  $\hat{c}_{i \in B, \sigma}$  as  $\hat{a}_{k\sigma}^\dagger$  and  $\hat{b}_{k\sigma}$  respectively:

$$\begin{aligned} \hat{c}_{i \in A, \sigma}^\dagger &= \frac{1}{\sqrt{N_s}} \sum_k \hat{a}_{k, \sigma}^\dagger e^{ik \cdot R_i}, \\ \hat{c}_{i \in B, \sigma} &= \frac{1}{\sqrt{N_s}} \sum_k \hat{b}_{k, \sigma} e^{ik \cdot R_i}. \end{aligned} \quad (7)$$

where  $N_s$  is the number of unite cells and  $k$  belong to the first Brillouin Zone of the honeycomb lattice. Now we substitute Eq.(6) and Eq.(7) into Eq.(1) we could get the momentum space form of  $H_{\text{KMH}}$ :  $H_{\text{KMH}}(k)$ . In the Nambu basis:  $\psi^\dagger(k) = (\hat{a}_{k\uparrow}^\dagger, \hat{a}_{-k\downarrow}^\dagger, \hat{b}_{k\uparrow}, \hat{b}_{-k\downarrow})$ ,  $H_{\text{KMH}}(k)$  could be casted into a matrix form in momentum space, that's:

$$H_{\text{KMH}}(k) = \sum_k \psi^\dagger(k) h(k) \psi(k) + UN_s |\Delta_s|^2 \quad (8)$$

with the  $4 \times 4$  matrix  $h(k)$ :

$$h(k) = \begin{pmatrix} C + D & -U\Delta_s & \gamma(k) & 0 \\ -U\Delta_s & -C - D & 0 & -\gamma(k) \\ \gamma^\dagger(k) & 0 & C - D & -U\Delta_s \\ 0 & -\gamma^\dagger(k) & -U\Delta_s & -C + D \end{pmatrix} \quad (9)$$

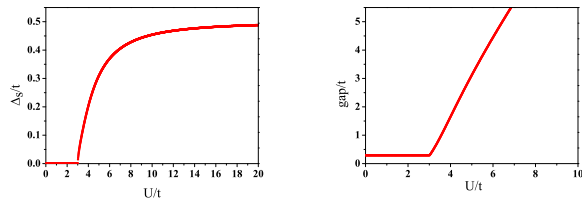


FIG. 4: (color online) (a) The mean field results of  $\Delta_s$  we solve from Eq.(11) at  $H_{\text{KMH}}$ 's flat-bands limit. (b) The excitation energy gap of the  $SC$  phase as a function of the interaction strength  $U$ , this excitation gap increases with  $U$  monotonically so there is no further topological phase transition upon varying  $U$ .

where  $C$  and  $D$  are the same as in Eq.(4). The quasi-particles spectrum can be found by diagonalize the Hamiltonian(9) in the momentum space:

$$E_n(k) = \pm\sqrt{e_1 \pm 2e_2}. \quad (10)$$

where

$$e_1 = C^2 + D^2 + |\gamma(k)|^2 + (U\Delta_s)^2, \\ e_2 = \sqrt{C^2 (D^2 + |\gamma(k)|^2)}.$$

We would investigate the instability of the  $TI$  phase of  $H_{\text{KMH}}$  in the presence  $SC$  fluctuation as the interaction strength  $U$  increases by minimizing the ground state's energy  $E_0 = \sum_{n,k} E_n(k)$  against the  $SC$  order parameters  $\Delta_s$ , i.e.,  $\partial E_0 / \partial \Delta_s = 0$ . Then the self-consistent mean field equation is given by:

$$1 = \frac{U}{2N_s} \sum_k \left( \frac{1}{E_1(k)} + \frac{1}{E_2(k)} \right). \quad (11)$$

where  $E_1(k) = -\sqrt{e_1 + 2e_2}$  and  $E_2(k) = -\sqrt{e_1 - 2e_2}$  are the two lowest filled bands in Eq.(10).

The mean field solution of the self-consistent equation Eq.(11) are plotted in Fig.4(a) from which we can see that beyond a critical value of the attractive interaction strength:  $U_c \simeq 3.03t$  the  $TI$  phase of the  $H_{\text{KMH}}$  model in its flat-bands limit become unstable against a  $SC$  phase transition.

The quasi-particles excitation gap in the  $SC$  phase increases with  $U$  monotonically, see Fig.4(b). This mean that there is no gap closing and no further topological phase transition upon varying  $U$ .

Fig.5 and Fig.6 is the mean filed results of the  $SC$  order parameter  $\Delta_s$  we obtained from solving Eq.(11) and the excitation gap of  $SC$  phase over a range of  $t'$  and  $U$  with the other parameters are fixed in the flat-bands limit. Note that in the presence of the bulk gap  $\Delta_{t'}$  the order parameter  $\Delta_s$  and the excitation gap of  $SC$  phase are not the same like in the traditional  $SC$  phase transition[17]. From Fig.5 we could infer that the critical

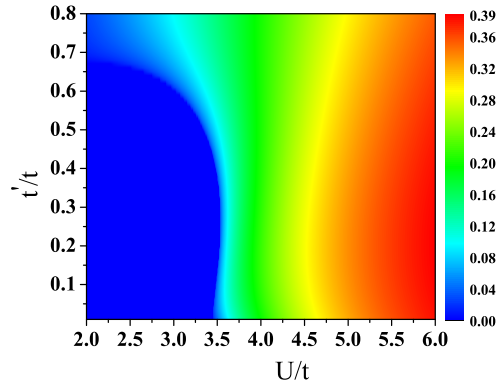


FIG. 5: (color online) The mean field results of the  $SC$  order parameter  $\Delta_s$  we solve from Eq.(11) over a range of  $U$  and  $t'$ , Other parameters are in the flat-bands limit.

interaction strength  $U_c$  which separate the  $TI$  and  $SC$  phase increases nearly linearly with  $t'$ .

As a consequence of TRS in  $H_{\text{KMH}}$ , the Chern number will be zero and we verified this by a numerical calculation. We calculate the Chern number of the two lowest bands of  $h(k)$  is  $h(k)$ [15, 16], the numerical results show that the total Chern number  $C = 0$  in the  $SC$  phase at  $U = 3.03$  with  $\Delta_s = 0.0147$  while the other parameters in the flat-bands limit. This mean that the  $SC$  phase transition destroy the TFBs. The topological property of this  $SC$  state can also be see from its edge excitations, so we also calculate the energy bands of  $H_{\text{KMH}}$  in a cylinder geometry. The numerical results are depicted in Fig.7 from which we can see that the edge states are gapped when the  $SC$  order is developed in  $H_{\text{KMH}}$ . So beyond the critical interaction strength  $U_c$ ,  $H_{\text{KMH}}$  entering a topological trivial  $SC$  phase. On the other hand, we found a pair finite-energy bound state in the energy spectrum if a pair of  $\pi$ -fluxes are inserted into the  $SC$  phase with periodic boundary condition in both  $x$  and  $y$  direction, see Fig.8, comparing with the  $\pi$ -flux-induced zero-energy modes in Fig.3 in the  $TI$  phase, show that the  $SC$  phase is topological trivial. This finite energy bound states and the gapped edge states in Fig.7 verified that the  $H_{\text{KMH}}$  model will loss its topology properties upon entering this s-wave  $SC$  phase as the attractive interaction strength increasing.

So the  $SC$  phase in  $H_{\text{KMH}}$  develops from a fully gapped  $TI$  state. This kind of  $SC$  phase transition is different from the traditional  $SC$  phase transition which develops from a Fermi liquid in which the low energy excitations are gapless. If a  $SC$  order is develops from an fully gapped state, in our case an  $TI$  state, there will be an kind of gapped excitations, the so called Cooperon, in the insulator side of this  $SC$  phase transition[17, 18]. This type of  $SC$  phase transition's mechanism could be understand in this way. There is a competition between the  $SC$  pairing gap  $\Delta_s$  and the topological energy gap  $\Delta_{t'}$  upon

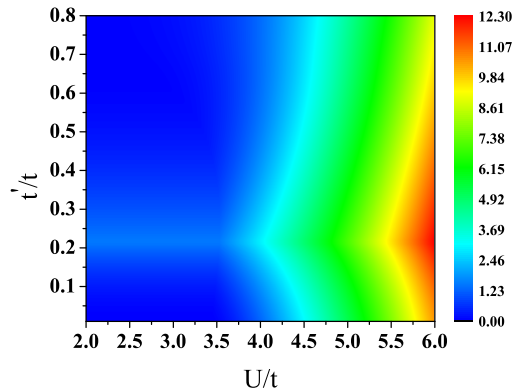


FIG. 6: (color online) The mean field results of the excitation energy gap in the  $SC$  phase over a range of  $U$  and  $t'$  while other parameters are in the flat-bands limit.

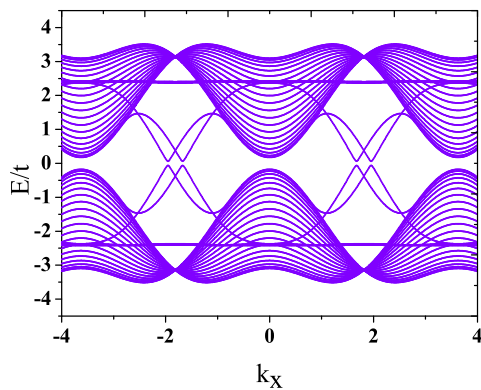


FIG. 7: (color online) Energy bands of  $H_{\text{KMH}}$  in its  $SC$  phase in a cylinder geometry with “zigzag” boundary. The  $SC$  phase is at  $U = 3.91$  with  $\Delta_s = 0.016t$ , the other parameters are in the flat-bands limit.

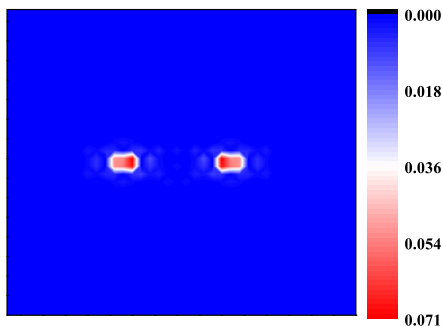


FIG. 8: (color online) The contour plots of the particle density distribution of the finite-energy bound states in the coordinate space. We can see that the finite-energy states are bound to the  $\pi$ -fluxes. The values of particle density are indicated by color.  $H_{\text{KMH}}$ 's in its  $SC$  phase and flat-bands limit.

the varying of interaction strength  $U$ . If the topological energy gap  $\Delta_{t'}$  is large enough, the Cooperon excitations will have an energy gap and will not condense, so the  $SC$  order parameter is vanishingly small. On the other hand, if  $\Delta_{t'}$  is very small or the  $SC$  energy gap is large enough (at large  $U$ ), the Cooperon excitations will become gapless and condensed, their condensation will lead to the  $SC$  phase transition at last.

#### IV. CONCLUSION

In this paper, we study the influence of attractive correlation on  $TI$  using the  $H_{\text{KMH}}$  model via a self-consistent mean field method. In the mean field level, we found a  $TI - SC$  phase transition upon increasing the attractive interaction strength  $U$  in this model. The mechanism leading to this  $SC$  phase transition is different from the traditional ones. There is a competition between the topological energy gap  $\Delta_{t'}$  and the  $SC$  energy gap before the  $SC$  phase transition. This competition is reflected in the gapped Cooperon excitation, when the  $SC$  pairing gap is larger than  $\Delta_{t'}$ , the Cooperon excitation will condense and the  $SC$  phase transition occurs in the system eventually. We think those results may help in better understanding the quantum exotic states in the correlated topological insulator and the pseudogap state in the high  $T_C$  cuprate superconductor[19].

**Acknowledgments.** we thank professor Su-Peng Kou for his many helpful advices. This research is supported by National Basic Research Program of China (973 Program) under the grant No. 2011CB921803, 2012CB921704 and NFSC Grant No.11174035.



- 
- [1] K. V. Klitzing, G. Dorda, and M. Pepper, Phys. Rev. Lett. 45, 494 (1980).
- [2] F. D. M. Haldane, Phys. Rev. Lett. 61, 2015 (1988).
- [3] D.J. Thouless, M. Kohmoto, M.P. Nightingale, and M. den Nijs, Phys. Rev. Lett. 49, 405 (1982).
- [4] D. Zheng, G.-M. Zhang, and C. Wu, Phys. Rev. B 84, 205121 (2011).
- [5] K. Sun, Z. Gu, H. Katsura, and S. Das Sarma, Phys. Rev. Lett. 106, 236803 (2011).
- [6] Yi Fei Wang, Zheng Cheng Gu, Chang De Gong, and D. N. Sheng, Phys. Rev. Lett. 107, 146803 (2011).
- [7] E. Tang, J.-W. Mei, and X.-G. Wen, Phys. Rev. Lett. 106, 236802 (2011).
- [8] B. A. Bernevig and S.-C. Zhang, Phys. Rev. Lett. 96, 106802 (2006).
- [9] C. L. Kane and E. J. Mele, Phys. Rev. Lett. 95, 146802 (2005).
- [10] D. C. Tsui, H. L. Stormer, and A. C. Gossard, Phys. Rev. Lett. 48, 1559 (1982).
- [11] Jie Yuan, Jin-Hua Gao, Wei-Qiang Chen, Fei Ye, Yi Zhou and Fu-Chun Zhang, Phys. Rev. B 86, 104505 (2012).
- [12] Dung-Hai Lee, Phys. Rev. Lett. 107, 166806 (2011).
- [13] Zi Yang Meng, Hsiang-Hsuan Hung, Thomas C. Lang. Modern Physics Letters B 28:01.(2014)
- [14] F. F. Assaad, M. Bercx, and M. Hohenadler, Phys. Rev. X 3, 011015 (2013).
- [15] R. Resta, Rev. Mod. Phys. 66, 899 (1994).
- [16] T. Fukui, Y. Hatsugai and H. Suzuki: J. Phys. Soc. Jpn. 74, 1674 (2005).
- [17] P. Nozières and F. Pistolesi, Eur. Phys. J. B 10, 649 (1999).
- [18] K.-Y. Yang, T. M. Rice, and F.-C. Zhang, Rep. Prog. Phys. 75, 016502 (2012).
- [19] Konik R, Rice T M and Tsvetik A M 2010 Phys. Rev. B 82, 054501.